

April 21, 2013 9:27

WSPC - Proceedings Trim Size: 9in x 6in scopetta

1

Sivers function in constituent quark models

S. Scopetta

Dipartimento di Fisica, Università degli Studi di Perugia, and INFN,
sezione di Perugia, via A. Pascoli, 06100 Perugia, Italy

A. Courtoy

Departament de Física Teòrica, Universitat de València and IFIC, CSIC
46100 Burjassot (València), Spain

F. Fratini

Dipartimento di Fisica, Università degli Studi di Perugia,
via A. Pascoli, 06100 Perugia, Italy

V. Vento

Departament de Física Teòrica, Universitat de València and IFIC, CSIC
46100 Burjassot (València), Spain,
TH-Division, PH Department, CERN, CH-1211 GENEVE 23, Switzerland

A formalism to evaluate the Sivers function, developed for calculations in constituent quark models, is applied to the Isgur-Karl model. A non-vanishing Sivers asymmetry, with opposite signs for the u and d flavor, is found; the Burkardt sum rule is fulfilled up to 2%. Nuclear effects in the extraction of neutron single spin asymmetries in semi-inclusive deep inelastic scattering on ^3He are also evaluated. In the kinematics of JLab, it is found that the nuclear effects described by an impulse approximation approach are under control.

Keywords: DIS, transversity, neutron structure.

1. The Sivers function in Constituent Quark Models

The partonic structure of transversely polarized nucleons is still an open problem.¹ Semi-inclusive deep inelastic scattering (SIDIS) is one of the proposed processes to access the parton distributions (PDFs) of transversely polarized hadrons. SIDIS of unpolarized electrons on a transversely polarized target shows "single spin asymmetries" (SSAs),² due to two physical mechanisms, whose contributions can be distinguished,^{3,5} i.e. the Collins² and

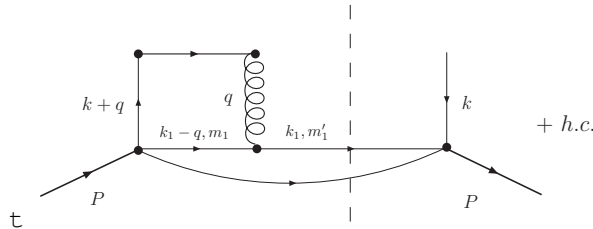


Fig. 1. The contributions to the Sivers function in the present approach.

the Sivers⁶ mechanism. The former is due to parton state interactions (FSI) in the production of a hadron by a transversely polarized quark. The Sivers mechanism leads to a SSA which is the product of the unpolarized fragmentation function with the Sivers PD. The latter describes the number density of unpolarized quarks in a transversely polarized target: it is a time-reversal odd, Transverse Momentum Dependent (TMD) PD. From the existence of leading-twist Final State Interactions (FSI),^{7,8} a non-vanishing Sivers function has been explained as generated by the gauge link in the definition of TMDs,^{9,10} whose contribution does not vanish in the light-cone gauge, as happens for the standard PD functions. Recently, the first data of SIDIS on transversely polarized targets have been published, for the proton¹¹ and the deuteron.¹² It has been found that, while the Sivers effect is sizable for the proton, it becomes negligible for the deuteron, so that apparently the neutron contribution cancels the proton one, showing a strong flavor dependence of the mechanism. Different parameterizations of the available SIDIS data have been published,¹³⁻¹⁵ still with large error bars. Since a calculation from first principles in QCD is not yet possible, several model evaluations have been performed, e.g. in a quark-diquark model,^{7,9,16} in the MIT bag model,¹⁷ in a light-cone model,¹⁸ in a nuclear framework, relevant to proton-proton collisions.¹⁹ We here describe a Constituent Quark Model (CQM) calculation of the Sivers function.²⁰ CQM calculations of PDs are based on a two steps procedure.²¹ First, the matrix element of the proper operator is evaluated using the wave functions of the model; then, a low momentum scale, $\frac{2}{0}$, is ascribed to the model calculation and QCD evolution is used to evolve the observable calculated in this low energy scale to the scale of DIS experiments. Such procedure has proven successful in describing the gross features of PDs²² and GPDs,²³ by using different CQMs, e.g. the Isgur-Karl (IK) model.²⁴ Besides the fact that it successfully reproduces the low-energy properties of the nucleon,

the IK model contains the one-gluon-exchange (OGE) mechanism.²⁵ In the present calculation, with respect to calculations of PDFs and GPDs, the leading twist contribution to the FSI has to be taken into account. The main approximations have been: i) only the valence quark sector is investigated; ii) the leading twist FSI are taken into account at leading, OGE, order, which is natural in the IK model; iii) the resulting interaction has been obtained through a non-relativistic (NR) reduction of the relevant operator, according to the philosophy of constituent quark models,²⁵ leading to a potential V_{NR} . The Sivers function for a proton polarized along the y axis and for the quark of flavor Q , $f_{1T}^{\perp Q}(x; k_T)$, takes the form (cf. Fig. 1 for the labels of the momenta and helicities):

$$f_{1T}^{\perp Q}(x; k_T) = ig^2 \frac{M^2}{k_x} \int d^3k_1 d^3k_3 \frac{d^2q_T}{(2\pi)^2} (k_3^+ - xP^+) (\vec{k}_{3T} + \vec{q}_T - \vec{k}_{1T}) M^Q \quad (1)$$

where g is the strong coupling constant, M the proton mass, and

$$M^{u(d)} = \sum_{m_1, m_3} \sum_{m_1^0, m_3^0} \sum_{s_f, s_z = \pm 1}^y \langle \vec{k}_3; m_3; \vec{k}_1; m_1; P \rangle \langle \vec{k}_3 - \vec{k}_1; m_n \rangle \frac{1}{2} V_{NR}(\vec{k}_1; \vec{k}_3; \vec{q}) \langle \vec{k}_3 + \vec{q}; m_3^0; \vec{k}_1 - \vec{q}; m_1^0; P \rangle \langle \vec{k}_3 - \vec{k}_1; m_n \rangle : \quad (2)$$

Using the spin-flavor wave function of the proton in momentum space, ψ_{sf} , corresponding to a given CQM, the Sivers function, Eq. (1), can be evaluated. From Eq. (2), one notices that the helicity conserving part of the global interaction does not contribute to the Sivers function. Besides, in an extreme NR limit, it turns out to be identically zero: in our scheme, it is precisely the interference of the small and large components in the four-spinors of the free quark states which leads to a non-vanishing Sivers function. This holds even from the component with $l=0$ of the target wave function. While, in other approaches,¹⁷ these interference terms arise due to the wave function, they are produced here by the interaction.

The above-described formalism is now applied to the IK model. The detailed procedure and the final expressions of the Sivers function in this model can be found in Ref.²⁰ To evaluate numerically Eq. (1), g (i.e. $\alpha_s(Q^2)$) has to be fixed. The prescription²¹ is used to fix $\alpha_s(Q^2)$, according to the amount of momentum carried by the valence quarks in the model. Here, assuming that all the gluons and sea pairs in the proton are produced perturbatively

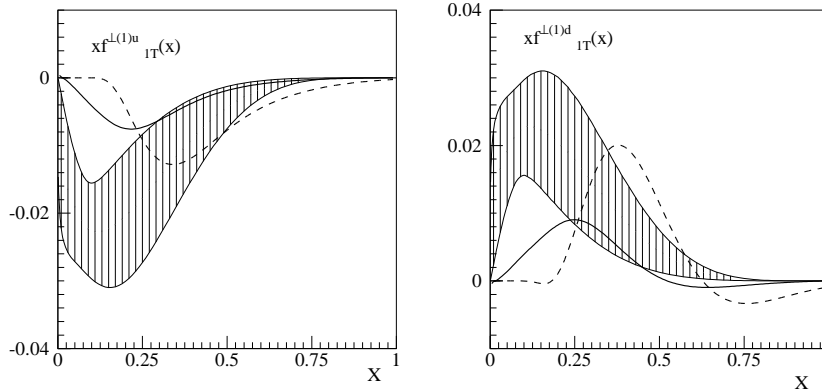


Fig. 2. Left (right): the quantity $f_{1T}^{(1)u(d)}$ (x), Eq. (3). Dashed curve: IK at Q_0^2 . Full curve: the evolved distribution at NLO. Patterned area: parameterization by¹⁴ (see text).

according to NLO evolution equations, in order to have $\int_0^1 x f_{1T}^{(1)u} dx = 0.55$ of the momentum carried by the valence quarks at a scale of 0.34 GeV^2 one finds that $Q_0^2 = 0.1 \text{ GeV}^2$ if $\frac{N_{CD}}{Q_{CD}} = 0.24 \text{ GeV}$. This yields $s(\frac{Q_0^2}{Q^2}) = (4) = 0.13$.²¹ The results of the present approach for the first moments of the Sivvers function, defined as

$$f_{1T}^{(1)Q} (x) = \int d^2 k_T \frac{k_T^2}{2M^2} f_{1T}^{(1)Q} (x; k_T) ; \quad (3)$$

are given by the dashed curves in Fig. 2. They are compared with a parameterization of the HERMES data, taken at $Q^2 = 2.5 \text{ GeV}^2$: The patterned area represents the 1 σ range of the best fit proposed in Ref.¹⁴ The magnitude of the results is close to that of the data, although they have a different shape: the maximum (minimum) is predicted at larger values of x. Actually Q_0^2 is much lower, $Q^2 = 2.5 \text{ GeV}^2$. A proper comparison requires QCD evolution of TMDPDFs, what is, to large extent, unknown. We nevertheless perform a NLO evolution of the model results assuming, for $f_{1T}^{(1)Q} (x)$, the same anomalous dimensions of the unpolarized PDFs. From the final result (full curve in Fig. 2), one can see that the agreement with data improves dramatically and the trend is reasonably reproduced at least for $x < 0.2$. Although the performed evolution is not exact, the procedure highlights the necessity of evolving the model results to the experiment scale and it suggests that the present results could be consistent with data, still affected by large errors.

Properties of the Sivvers function can be inferred from general principles.

The Burkardt Sum Rule (BSR)²⁶ states that, for a proton polarized in the positive y direction, $\int_{-1}^1 h_{x^i}^Q = 0$ with

$$h_{x^i}^Q = \int_0^1 dx \int_{-1}^1 dk_T \frac{k_x^2}{M} f_{1T}^{?Q}(x; k_T); \quad (4)$$

and must be satisfied at any scale. Within our scheme, at the scale of the model, it is found $h_{x^i}^u = 10.85 \text{ MeV}$, $h_{x^i}^d = 11.25 \text{ MeV}$ and, in order to have an estimate of the quality of the agreement of our results with the sum rule, we define the ratio $r = \int h_{x^i}^d + h_{x^i}^u - \int h_{x^i}^d - h_{x^i}^u$ obtaining $r \approx 0.02$, so that we can say that our calculation fulfills the BSR to a precision of a few percent. One should notice that the agreement which is found is better than that found in other model calculations,^{16,17} especially for what concerns the fulfillment of the Burkardt Sum Rule.

2. The Sivers function from neutron (³He) targets

As explained in the previous section, the experimental scenario which arises from the analysis of SIDIS on transversely polarized proton and deuteron targets^{11,12} is puzzling. The data show an unexpected flavor dependence in the azimuthal distribution of the produced pions. With the aim at extracting the neutron information to shed some light on the problem, a measurement of SIDIS on transversely polarized ³He has been addressed,²⁷ and two experiments, aimed at measuring the azimuthal asymmetries in the production of leading pions from transversely polarized ³He, are forthcoming at JLab.²⁸ Here, a realistic analysis of SIDIS on transversely polarized ³He²⁹ is described. The expressions of the Collins and Sivers contributions to the azimuthal Single Spin Asymmetry (SSA) for the production of leading pions have been derived, in impulse approximation (IA), including the initial transverse momentum of the struck quark. The final equations are involved and they are not reported here. They can be found in.²⁹ The same quantities have been then evaluated in the kinematics of the JLab experiments. Wave functions³⁰ obtained within the AV18 interaction³¹ have been used for a realistic description of the nuclear dynamics, using overlap integrals evaluated in Ref.³² and the nucleon structure has been described by parameterizations of data or model calculations.^{13,33} The crucial issue of extracting the neutron information from ³He data will be now discussed. As a matter of facts, a model independent procedure, based on the realistic evaluation of the proton and neutron effective polarizations in ³He,³⁴ called respectively p_p and p_n in the following, is widely used in DIS to take into account effectively the momentum and energy distributions of the bound nucleons in

6

³He. It is found that the same extraction technique can be applied also in the kinematics of the proposed experiments, although fragmentation functions, not only parton distributions, are involved, as it can be seen in Figs. 1 and 2. In these figures, the free neutron asymmetry used as a model in the calculation, given by a full line, is compared with two other quantities. One is:

$$A_n^i \approx \frac{1}{d_n} A_3^{\text{exp};i} \quad ; \quad (5)$$

where *i* stands for "Collins" or "Sivers", $A_3^{\text{exp};i}$ is the result of the full calculation, simulating data, and d_n is the neutron dilution factor. The latter quantity is defined as follows, for a neutron *n* (proton *p*) in ³He:

$$d_{n(p)}(x; z) = \frac{\sum_q e_q^2 f^{q;n(p)}(x) D^{q;h}(z)}{\sum_{N=p,n} \sum_q e_q^2 f^{q;N}(x) D^{q;h}(z)} \quad (6)$$

and, depending on the standard parton distributions, $f^{q;N}(x)$, and fragmentation functions, $D^{q;h}(z)$, is experimentally known (see²⁹ for details). A_n^i is given by the dotted curve in the figures. The third curve, the dashed one, is given by

$$A_n^i \approx \frac{1}{p_n d_n} A_3^{\text{exp};i} - 2p_p d_p A_p^{\text{exp};i} \quad ; \quad (7)$$

i.e. ³He is treated as a nucleus where the effects of its spin structure, of Fermi motion and binding, can be taken care of by parameterizing p_p and p_n . One should realize that Eq. (5) is the relation which should hold between the ³He and the neutron SSA's if there were no nuclear effects, i.e. the ³He nucleus were a system of free nucleons in a pure S wave. In fact, Eq. (5) can be obtained from Eq. (7) by imposing $p_n = 1$ and $p_p = 0$. It is clear from the figures that the difference between the full and dotted curves, showing the amount of nuclear effects, is sizable, being around 10 - 15 % for any experimentally relevant *x* and *z*, while the difference between the dashed and full curves reduces drastically to a few percent, showing that the extraction scheme Eq. (7) takes safely into account the spin structure of ³He, Fermi motion and binding effects. This important result is due to the kinematics of the JLab experiments, which helps in two ways. First of all, to favor pions from current fragmentation, *z* has been chosen in the range 0.45 < *z* < 0.6, which means that only high-energy pions are observed. Secondly, the pions are detected in a narrow cone around the direction of the momentum transfer. As it is explained in²⁹ this makes nuclear effects in the fragmentation functions rather small. The leading nuclear effects

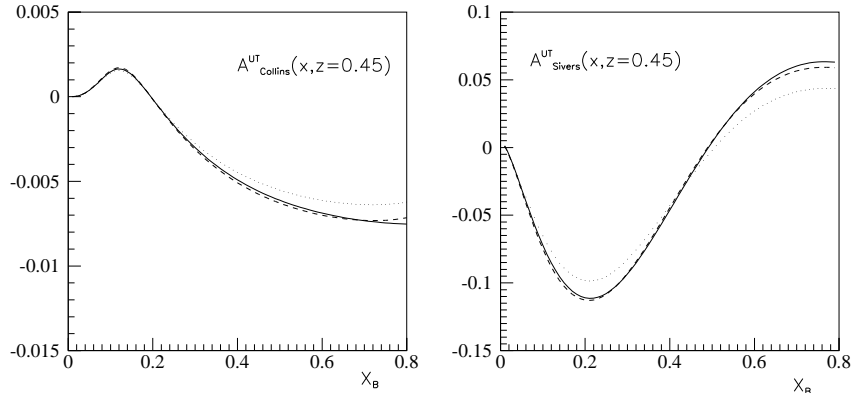


Fig. 3. Left (right) The model neutron Collins (Sivers) asymmetry for π^+ production (full) in JLab kinematics, and the one extracted from the full calculation taking into account the p_p (dashed), or neglecting it (dotted). The results are shown for $z = 0.45$ and $Q^2 = 2.2 \text{ GeV}^2$, typical values in the kinematics of the JLab experiments.

are then the ones affecting the parton distributions, already found in DIS, and can be taken into account in the usual way, i.e., using Eq. (7) for the extraction of the neutron information. In the figures, one should not take the shape and size of the asymmetries seriously, being the obtained quantities strongly dependent on the models chosen for the unknown distributions.³³ One should instead consider the difference between the curves, a model independent feature which is the most relevant outcome of the present investigation. Eq. (7) is therefore a valuable tool for the experiments.²⁸ The evaluation of final state interactions effects and the inclusion of more realistic models of the nucleon structure are in progress.

Acknowledgments

This work is supported in part by the INFN-CICYT agreement, by the Generalitat Valenciana under the contract AINV06/118; by the Sixth Framework Program of the European Commission under the Contract No. 506078 (I3 Hadron Physics); by the MEC (Spain) (FPA 2007-65748-C02-0, AP2005-5331 and PR2007-0048).

References

1. V. Barone, A. Drago and P. Ratcliffe, Phys. Rept. 359 1 (2002).
2. J. C. Collins, Nucl. Phys. B 396, 161 (1993).

3. P. J. Mulders and R. D. Tangerman, Nucl. Phys. B 461 (1996) 197.
4. A. M. Kotzinian and P. J. Mulders, Phys. Lett. B 406 (1997) 373.
5. D. Boer and P. J. Mulders, Phys. Rev. D 57 (1998) 5780; A. Bacchetta et al, JHEP 0702, 093 (2007).
6. D. W. Sivers, Phys. Rev. D 41, 83 (1990).
7. S. J. Brodsky et al, Phys. Lett. B 530, 99 (2002).
8. S. J. Brodsky et al, Phys. Rev. D 65, 114025 (2002).
9. J. C. Collins, Phys. Lett. B 536, 43 (2002); X. d. Ji and F. Yuan, Phys. Lett. B 543, 66 (2002); A. V. Belitsky et al, Nucl. Phys. B 656, 165 (2003).
10. A. D. Rago, Phys. Rev. D 71, 057501 (2005).
11. A. Arapetian et al, Phys. Rev. Lett. 94, 012002 (2005).
12. V. Y. Alexakhin et al, Phys. Rev. Lett. 94, 202002 (2005).
13. M. Anselmino et al, Phys. Rev. D 72, 094007 (2005).
14. J. C. Collins et al, Phys. Rev. D 73, 014021 (2006).
15. W. Vogelsang and F. Yuan, Phys. Rev. D 72, 054028 (2005).
16. L. P. Gamberg et al, Phys. Rev. D 67, 071504(R) (2003); A. Bacchetta et al, Phys. Lett. B 578, 109 (2004); A. Bacchetta et al, arXiv:0807.0323 [hep-ph].
17. F. Yuan, Phys. Lett. B 575, 45 (2003); I. O. Cherednikov et al, Phys. Lett. B 642, 39 (2006).
18. Z. Lu and B. Q. Ma, Nucl. Phys. A 741, 200 (2004).
19. A. Bianconi, arXiv:hep-ph/0702186.
20. A. Courtoy, F. Frattini, S. Scopetta, V. Vento, Phys. Rev. D (2008), in press; arXiv:0801.4347 [hep-ph].
21. M. Traini et al, Nucl. Phys. A 614, 472 (1997).
22. S. Scopetta and V. Vento, Phys. Lett. B 424, 25 (1998).
23. S. Scopetta and V. Vento, Eur. Phys. J. A 16, 527 (2003); S. Boer, B. Pasquini and M. Traini, Nucl. Phys. B 649, 243 (2003).
24. N. Isgur and G. Karl, Phys. Rev. D 18, 4187 (1978).
25. A. De Rujula et al, Phys. Rev. D 12, 147 (1975).
26. M. Burkardt, Phys. Rev. D 69 (2004) 091501.
27. S. J. Brodsky and S. Gardner, Phys. Lett. B 643 (2006) 22.
28. E-06-010 Proposal to JLab-PAC 29, J.-P. Chen and J.-C. Peng Spokespersons; E-06-011 Proposal to JLab-PAC 29, E. C. Isbani and H. Gao Spokespersons.
29. S. Scopetta, Phys. Rev. D 75, 054005 (2007).
30. A. K. Kievsky et al, Nucl. Phys. A 577, 511 (1994).
31. R. B. Wiringa et al, Phys. Rev. C 51 (1995) 38.
32. A. K. Kievsky et al, Phys. Rev. C 56, 64 (1997); E. Pace et al, Phys. Rev. C 64, 055203 (2001).
33. D. Amath et al, Phys. Rev. D 71, 114018 (2005).
34. C. Ciob degli Atti et al, Phys. Rev. C 48, 968 (1993).